

Experimental and Numerical Investigation on Design Optimization of a Roof Skylight Combined with Solar Chimney



Anon Anan-archa¹, Preeda Chantawong^{1*}, Joseph Khedari²

¹ Energy Engineering Technology Program, Department of Power Engineering Technology, College of Industrial Technology, King Mongkut's University of Technology North Bangkok, Wongsawang, Bangsue, Bangkok 10800, Thailand

² Division of Industrial Technology, Faculty of Science and Technology, Bangkokthonburi University, Taweewattana, Bangkok 10170, Thailand

Corresponding Author Email: preedac@kmutnb.ac.th

<https://doi.org/10.18280/ijht.410327>

ABSTRACT

Received: 17 April 2023

Accepted: 19 June 2023

Keywords:

roof design, skylight solar chimney, thermal performance, natural ventilation, daylight heat gain admission

The integration of roof skylight and solar chimney can provide daylight, induce ventilation, and reduce heat gain admission. This paper reports experimental and numerical investigation to determine the optimum design of a new roof configuration we introduced recently combining skylight with solar chimney (SSC). SSC is composed of a clear acrylic layer on the top, an intermediate layer composed of a set of distanced aluminium slats and a third layer composed of a combination of clear acrylic and aluminium slats. More precisely, we focus on the optimal position of the intermediate layer. Experimental investigation was conducted using two small rooms of 2.52 m³ volume built using commercial materials. The 30 degrees south facing roof included 0.50 m × 1.50 m × 0.15 m (W × L × H) SSC unit. A 0.025 m² outlet opening was located at the top lateral side and another inlet opening of similar surface area was installed on the bottom lower layer inside the room for ventilation. The first room, used as a reference, included SSC with intermediate layer located at the middle between the top and lower layers. Whereas in the second room, the position of intermediate was varied to be near the top layer (second configuration) and near the lower layer (third configuration). Solidworks flow simulation software package is used to simulate the thermal performance of SSC. Field tests and numerical simulations results showed that the position of intermediate layer did not affect indoor temperature significantly as temperatures were not much different. However, lowest heat flux transmitted through SSC and lower illuminance are observed when located near the lower layer. The induced air change was relatively similar for the three positions considered. Therefore, it is recommended that for practical application, the appropriate position for SSC intermediate layer should be located between the middle and lower layer as it will lead to good ventilation rate, lower indoor temperature, and less heat gain transmission without glare.

1. INTRODUCTION

Residences and buildings that are already in use often suffer from insufficient lighting and heat accumulation, especially on the top floor in the central part of the home or building. Reducing heat build-up is a top priority for tropical buildings. Natural ventilation is the most interesting method, especially for cooling the accumulated heat inside the attic and the building as it is simple and inexpensive. The integration of design concepts such as natural ventilation, passive design, natural daylighting to improve the thermal comfort of buildings was extensively investigated. Low-energy, zero-energy and green building concepts have attracted significant attention from architects and building technology designers due to the environmental concern of global warming. The literature is rich, and a complete review is out the space of this paper. By far, solar chimneys have been constantly studied and developed for several decades. Both roof and wall solar chimneys received considerable interest to induce ventilation, generate air movement inside the homes and buildings and reduce heat gain admission. Appropriate design of residences

and buildings in harmony with the environment and the climate is crucial for thermal comfort [1-3]. Several roofs [4-6] walls [6, 7] and double skin facades [8-10] configurations were introduced. Green facades to control wall surface temperature in buildings were investigated [11]. Day lighting and thermal analysis using various double reflective window glasses for green energy buildings was discussed [12]. Also, numerous investigations on the effect of the parameters of solar chimney have been carried out because they are critical for the fluid flow and heat transfer in solar chimney [cavity 13-19]. Other studies considered the development of roof solar chimney combined with other technologies such as evaporative cooling [20, 21], radiant barrier [22, 23], cool ceiling [24], earth to air heat exchanger [25], and water spraying [26]. Aforementioned papers provide several useful information such as the gap of solar chimney, thermal analysis, modelling, heat gain reduction and efficiencies. However, intergating skylight and solar chimney received less attention.

In a recent paper [27], we introduced a new roof configuration combining skylight with solar chimney referred to as SSC. It is composed of three layers: The top layer is made

from clear acrylic layer whereas the lower layer is composed of a combination of clear acrylic and aluminum slats. The intermediate layer is composed of distanced aluminum slats. SSC is intended to act as a solar chimney and allow daylight admission. This paper's aim is to conduct experimental and numerical investigation to determine the optimum position of the intermediate layer with respect to application in residences and buildings. Field tests are conducted using two small rooms built using commercial materials available in the local market whereas Solidworks flow simulation software package is used to simulate the thermal performance of SSC.

2. RESEARCH METHODOLOGY

Figure 1 (left) shows layers and dimensions of the SSC configuration, referred to as SSC-A, with intermediate layer located at the middle between the top and lower layers. The top layer of SSC is made from 3 mm clear acrylic layer whereas the lower layer is composed of a combination of 1mm clear acrylic and aluminium slats. To assess the effect of position on the intermediate layer and due to cost limitation, we used two small rooms of 2.52 m³ volume built using

commercial concrete blocks for walls and corrugated cement panels for roof [27] available in the market and widely used in the construction sector in the country. Figure 1 (right), shows schematic plan and elevation with dimensions of the experimental houses. The 30 degrees south facing roof of the first room used as a reference included SSC with intermediate layer located at the middle (SSC-A configuration) with the dimensions of 0.50 m × 1.50 m × 0.15 m (W × L × H). An outlet opening of 0.025 m² (0.05 m × 0.50m) was located at the top lateral side whereas another one of similar surface area was installed on the bottom lower layer inside the room for induced air ventilation. In the second room, the position of intermediate was varied to be near the lower layer (SSC-B configuration) and near the top layer (SSC-C configuration). SSC external sides were made from 1 mm thick aluminium sheet. Figure 2 shows perspective and section view of the three positions of the intermediate layer.

Temperatures at different positions of SSC, heat transferred through SSC, indoor illuminance and ambient conditions were measured continuously following the methodology adopted in [27]. For more details about experimental procedure, measuring devices and materials properties, please refer to information reported [27].

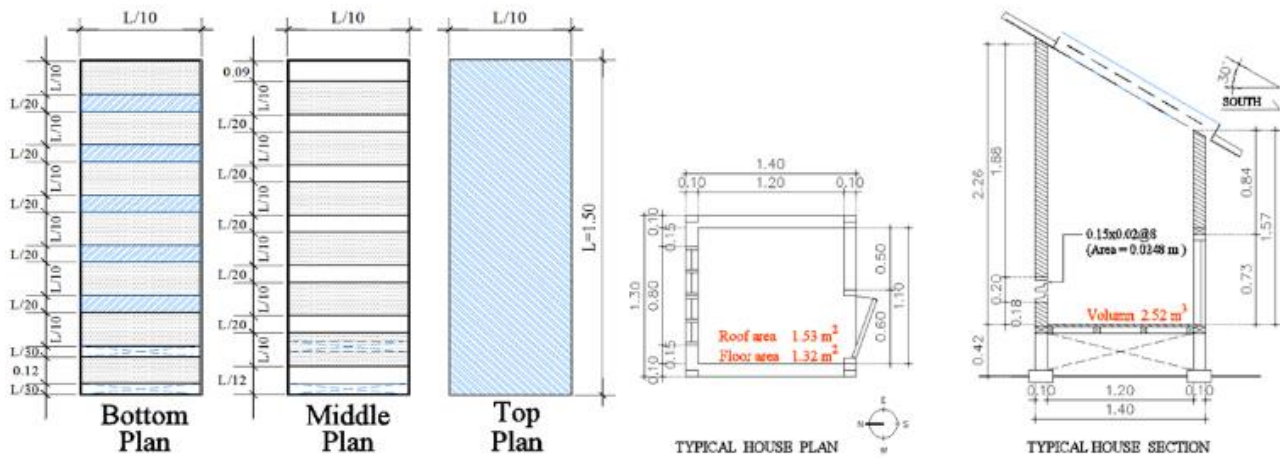


Figure 1. Plans and dimensions of the SSC-A (left) and plan and section of the experimental house model (right)

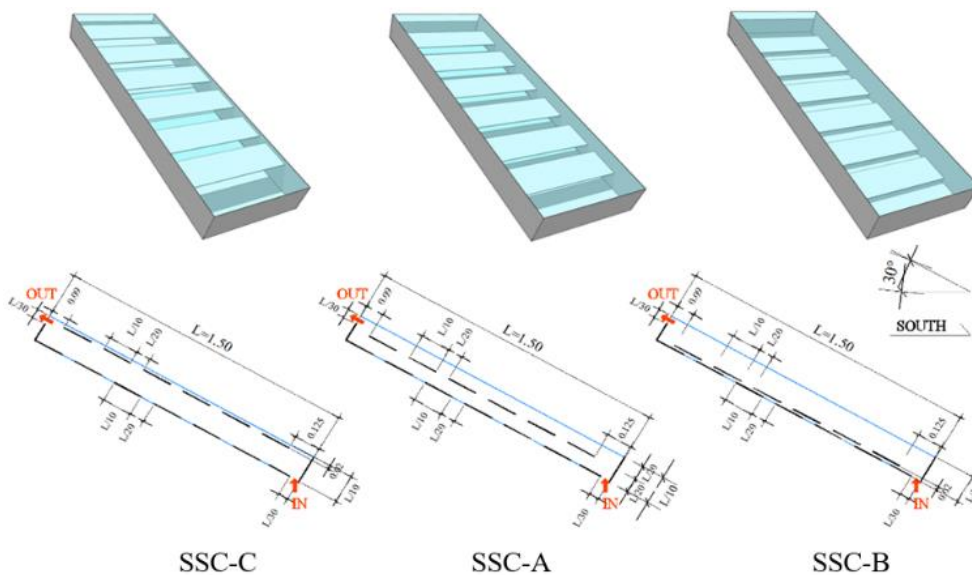


Figure 2. Perspectives and section views of the three configurations simulated

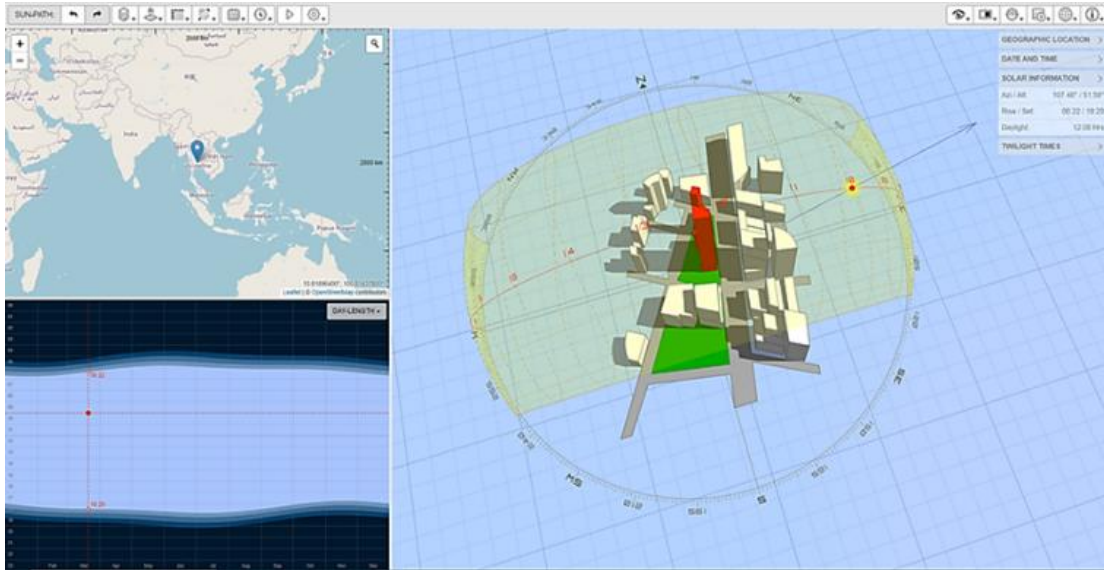


Figure 3. The solar data derived from the website and sun position at 10 a.m., June 21, 2021. (<http://andrewmarsh.com/software/sunpath3d-web/>)

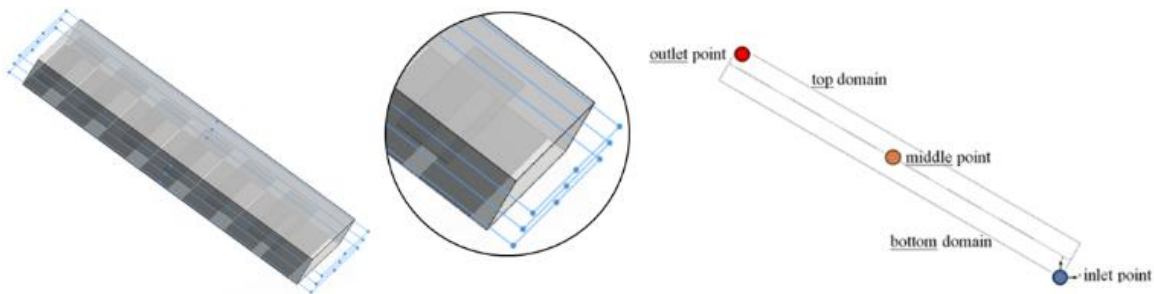


Figure 4. The planes used to observe behavior (left) and air velocity (right)

We used Solidworks flow simulation software package licensed by the university to simulate the thermal performance of SSC as it is easy to use and applicability to simulate SSC configuration. The thermal properties of solid materials are given in the study [27]. The fluid is air and the time increment is 36 second. The orbital direction of the sun can be determined by taking the coordinates of the site considered for simulation from Google earth pro and then inserting the data into <http://andrewmarsh.com/software/sunpath3d-web>. For the numerical simulation, we use the coordinates of the site located in Samut Sakhon province, southwest of Bangkok (Nadee Subdistrict, Samut Sakhon, latitude 13.606342, longitude 100.3143494). The date used in the analysis is June 2021. We choose this as it is a day with ambient conditions frequent in the country. In this day, the sun moves from east to west with a slight angle to the south. The Sun direction movement of this coordinate at 10:00 am is shown in Figure 3. Figure 4 shows the planes used to observe behavior and air velocity.

3. RESULTS AND DISSCUSION

Filed tests were conducted during several days. Data was recorded from 6:00 a.m.to 6:00 p.m. Although ambient conditions were not the same, subjective analysis and reasonable comparison using measured data could be made. In the first series, we compared the thermal performance between the SSC-A and SSC-B whereas in the second, SSC-A

performances are compared with SSC-C.

3.1 Room temperature

Figure 5 shows comparison between the hourly variation of room temperature measured at the center of room at 0.95cm high from the floor of SSC-A and SSC-B (left) and SSC-A and SSC-C (right). It can be observed that the temperature in the SSC-A house was lower than that of SSC-B in the morning 6:00-9:30 a.m. This is a result of better heat exchange between SSC, indoor and the surrounding due to the position of intermediate layer compared to that of SSC-B. Then it increased with the increasing intensity of incident solar radiation and higher temperature than SSC-B is recorded and non negligible difference is observed. This is again due the position of intermediate layer that allow higher heat from the incident radiation to penetrate to the indoor space through the SSC with higher heat accumulation in configuration SSC-A compared to SSC-B. In the afternoon, when the incident solar radiation started to decrease, negligible temperature difference between the two configurations is observed. At 16:00, the SSC-A room temperature was significantly lower compared to that of SSC-B. This is due to better heat exchange with the environment like in the morning hours.

Data analysis of the second series indicates that the indoor temperature in the morning until 1p.m. of both of SSC-A and SSC-C were similar (Figure 5, right) expect the first hour in the morning. After that time, it is observed that the temperature of SSC-C was higher than that of SSC-A until 18:00 p.m. This

is due to the high position of intermediate layer that leads to higher incident heat transmission compared to SSC-A. However, as the measured temperatures differences are not that much different, it is reasonable to conclude that the position of intermediate layer did not affect indoor temperature significantly.

3.2 Heat flux

Comparison of the measured heat flux transmitted through SSC between the two series of field tests is shown in Figure 6.

It can be observed that the measured heat flux followed well the incident solar radiation. The higher is the incident solar intensity and the higher the measured heat flux. Due to the position of intermediate layer near the bottom, the measured heat flux transmitted through SSC-B is always lower than that of SSC-A (Figure 6 left) with significant difference around noon. Whereas, in the second series of measurement, heat flux transmitted through SSC-A is always lower than that of SSC-C (Figure 6 right) but with smaller difference when compared to the first set of measurement.

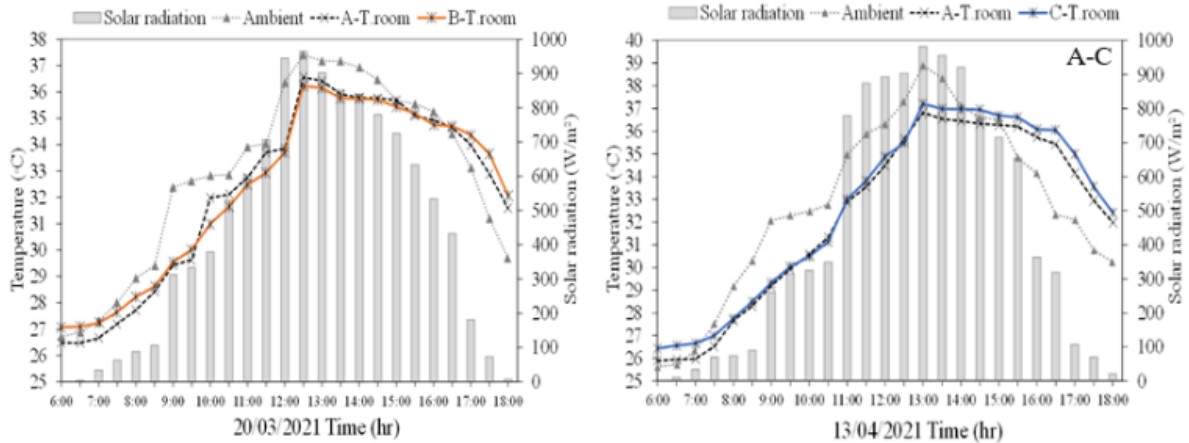


Figure 5. Comparison of hourly variation room temperature between SSC-A and SSC-B (left) and SSC-A and SSC-C (right)

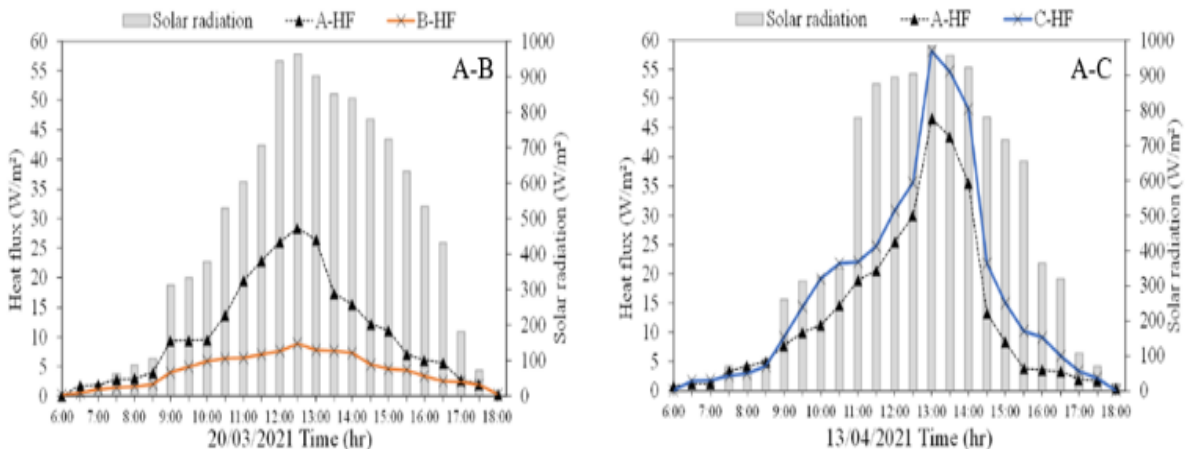


Figure 6. Hourly variation of heat flux transmitted of SSC-A and SSC-B (left) compared with SSC-A and SSC-C (right)

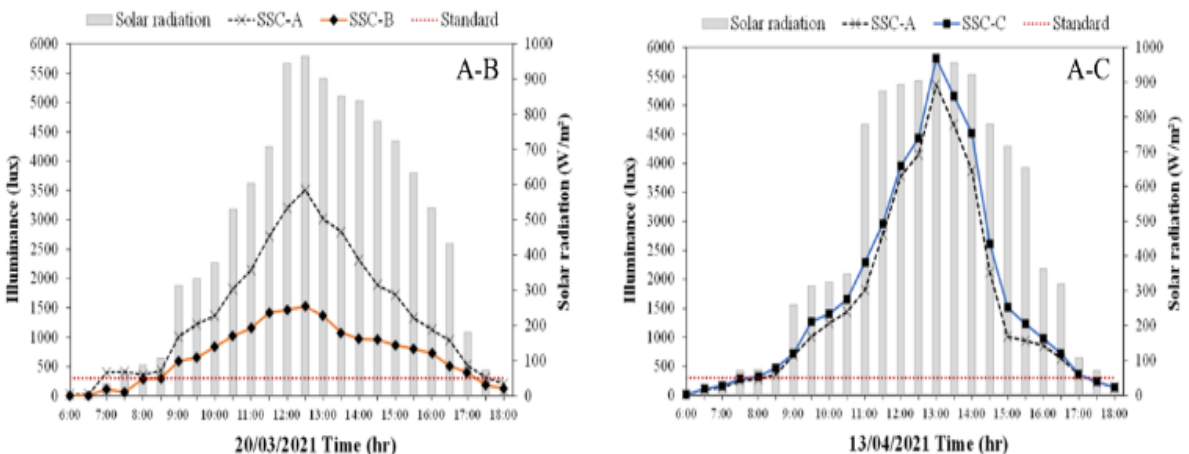


Figure 7. Hourly variation of the indoor illuminance of SSC-A and SSC-B (left) compared with SSC-A and SSC-C (right)

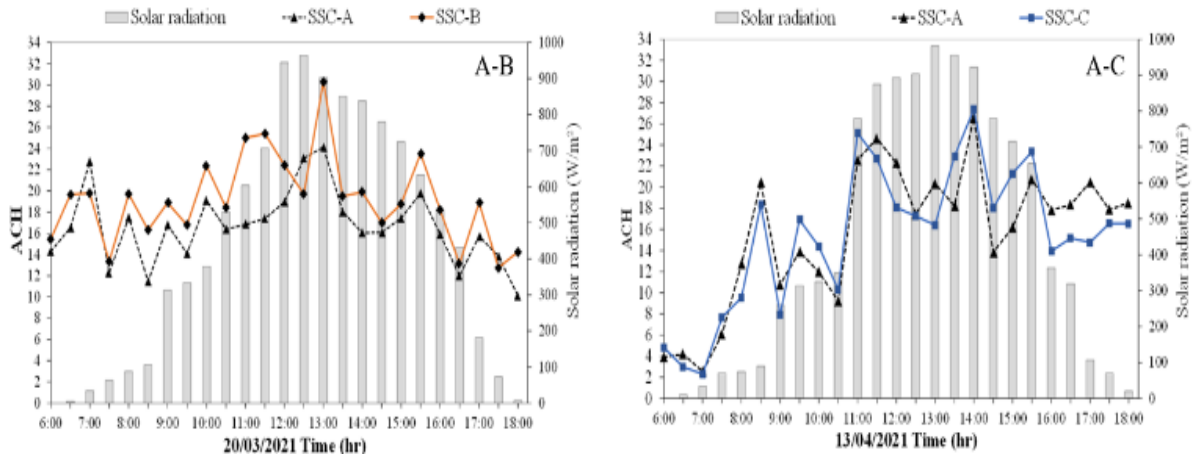


Figure 8. Hourly variation the measured air change of SSC-A and SSC-B compared with SSC-A and SSC-C

Table 1. Maximum, minimum, and average ACH of SSC-A, SSC-B and SSC-C on 20 March 2021 and 13 April 2021

20 March 2021	SSC-A	SSC-B	13 April 2021	SSC-A	SSC-C
Min	10.120	12.770	Min	2.543	2.312
Max	24.135	30.325	Max	26.590	27.372
Ave	16.667	19.186	Ave	15.667	15.390

3.3 Indoor illuminance

The measured hourly variation the indoor illuminance of SSC-A and SSC-B and SSC-A and SSC-C are shown in Figure 7. It varied like the measured heat flux and the higher is the position of the intermediate layer, the higher the indoor illuminance. Therefore, and under test conditions, locating the intermediate layer between the middle and lower layer is recommended to avoid excessive indoor illuminance that exceeds the recommended 300 lux standard.

3.4 Room air change

Plots of the measured induced air change (ACH) induced by the three configurations of SSC are shown in Figures 8. Obviously, this induced air change by SSC is also affected by natural wind. Maximum, minimum, and average ACH are listed in Table 1.

It can be seen that the average ACH of SSC-A was lower than SSC-B but higher than SSC-C. This is evident due to the position of intermediate layer. In configuration SSC-B, practically all incident solar radiation is trapped inside the SSC that increases the air temperature leading therefore to higher induced ventilation rate. The opposite is true for configuration SSC-C.

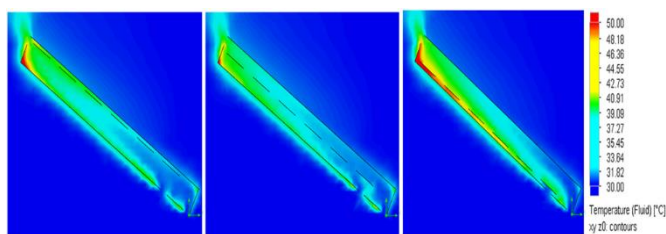


Figure 9. Temperature distribution across the section of SCC with upper, middle and lower position of intermediate layer

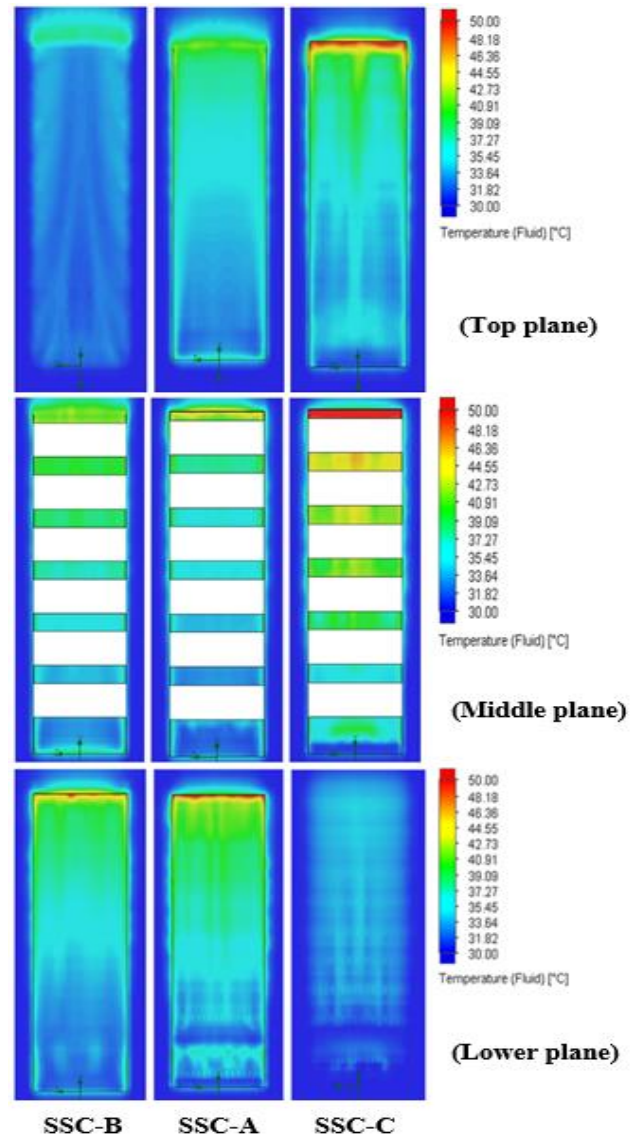


Figure 10. Temperature distribution at the top, middle and lower planes of the three positions of intermediate layers

3.5 Numerical results

Figure 9 shows the temperature distribution across the section of SCC-B, SCC-A, and SCC-C whereas Figure 10 shows the temperature distribution at the top plane, middle and bottom planes of SSC for the three positions of intermediate layer considered. Simulation results showed that installing the intermediate layer near the top leads to lowest temperatures compared to the other configurations. The maximum average temperature of SSC occurred around 13:30 pm is 54.82°C 57.15°C and 59.50°C for the upper, middle and lower position of intermediate layer respectively.

Similarly, the simulated daily average air temperature for the three positions of intermediate layer at the inlet, middle and outlet positions of SSC are given in Table 2. Obviously, these temperatures varied like the temperature distribution of measured discussed earlier and the highest air temperatures are observed when the intermediate layer was located near the bottom layer (SSC-B). It worth to mention that detailed comparison between measured and simulated results might not be appropriate due to limitation of measured data compared to simulated ones. However, subjective comparisons indicate that these observations agreed well with experimental results that validate our results and our choice of using solid works simulation software package. Consequently, it can be used to design SSC with respect to practical application and integration in building.

Table 2. The average daily air temperature of the three positions of intermediate layer at the inlet, middle and outlet of SSC

Configuration	Daily Average Temperature °C		
	Inlet-Avr.	Middle-Avr.	Outlet-Avr.
SSC-B	40.59	43.75	45.31
SSC-A	41.53	45.24	48.11
SSC-C	42.58	47.07	49.58

4. CONCLUSION

Numerical and experimental investigation of the performance of roof configuration combining skylight with solar chimney (SSC) composed of a clear acrylic layer on the outer side, a set of aluminium slats distanced each other located inside, and a combination of clear acrylic and aluminium slats at the inner side are reported and discussed. In term of thermal performance of SSC, results showed that the position of intermediate layer did not affect indoor temperature significantly as temperatures were relatively close and the induced air change was relatively similar for the three positions considered. However, when considering daylighting, the lowest heat flux transmitted through SSC and lower indoor illuminance are observed when located near the lower layer. Therefore, it is recommended that for building integration the intermediate layer be located between the middle and the bottom layer for better thermal performance in term of ventilation, heat gain reduction and lower glare. Adjustment of its position can be made depending on architectural requirement and desired daylight control.

Exploring the effects of use of different materials, geometries, or climatic conditions on the performance of SSCs deserves further investigation.

REFERENCES

- [1] Oktay, D. (2002). Design with the climate in housing environments: An analysis in Northern Cyprus. *Building and Environment*, 37(10): 1003-1012. [https://doi.org/10.1016/S0360-1323\(01\)00086-5](https://doi.org/10.1016/S0360-1323(01)00086-5)
- [2] Langer, S., Beko, G., Bloom, E., Widheden, A., Ekberg, L. (2015). Indoor air quality in passive and conventional new houses in Sweden. *Building and Environment*, 93: 92-100. <https://doi.org/10.1016/j.buildenv.2015.02.004>
- [3] Figueiredo, A., Figueira, J., Vicente, R., Maio, R. (2016). Thermal comfort and energy performance: Sensitivity analysis to apply passive house concept to the Portuguese climate. *Building and Environment*, 103: 276-288. <https://doi.org/10.1016/j.buildenv.2016.03.031>
- [4] Lei, Y., Zhang, Y., Wang, F., Wang, X. (2016). Enhancement of natural ventilation of a novel roof solar chimney with perforated absorber plate for building energy conservation. *Applied Thermal Engineering*, 107: 653-661. <https://doi.org/10.1016/j.applthermaleng.2016.06.090>
- [5] Bianco, V., Diana, A., Manca, O., Nardini, S. (2018). Numerical investigation of an inclined rectangular cavity for ventilated roofs applications. *Thermal Science and Engineering Progress*, 6: 426-435. <https://doi.org/10.1016/j.tsep.2018.02.016>
- [6] Thateenaranon, P., Amornkitbamrung, M., Hirunlabh, J., Khedari, J., Waewsak, J. (2017). Full-scale field investigation of a bio-climatic house under Thailand tropical climate. *Building and Environment*, 126: 54-67. <https://doi.org/10.1016/j.buildenv.2017.09.027>
- [7] Punyasompun, S., Hirunlabhm, J., Khedari, J., Zeghmata, B. (2009). Investigation on the application of solar chimney for multi-storey buildings. *Renewable Energy*, 34(12): 2545-2561. <https://doi.org/10.1016/j.renene.2009.03.032>
- [8] Souza, L.C.O., Souza, H.A., Rodrigues, E.F. (2018). Experimental and numerical analysis of a naturally ventilated double-skin façade. *Energy and Buildings*, 165: 328-339. <https://doi.org/10.1016/j.enbuild.2018.01.048>
- [9] Blanco, J.M., Arriaga, P., Rojí, E., Cuadrado, J. (2014). Investigating the thermal behavior of double-skin perforated sheet façades: Part A: Model characterization and validation procedure. *Building and Environment*, 82: 50-62. <https://doi.org/10.1016/j.buildenv.2014.08.007>
- [10] Blanco, J.M., Buruagaa, A., Cuadrado J., Zapicoc, A. (2019). Assessment of the influence of facade location and orientation in indoor environment of double-skin building envelopes with perforated metal sheets. *Building and Environment*, 163: 106325. <https://doi.org/10.1016/j.buildenv.2019.106325>
- [11] Vox, G., Blanco, I., Schettini, E. (2018). Green facades to control wall surface temperature in buildings. *Building and Environment*, 129: 154-166. <https://doi.org/10.1016/j.buildenv.2017.12.002>
- [12] Gorantla K.K., Shaik S., Setty A.B.T.P.R. (2018). Day lighting and thermal analysis using various double reflective window glasses for green energy buildings, *International Journal of Heat and Technology*, 36(3): 1121-1129. <https://doi.org/10.18280/ijht.360345>
- [13] Sakonidou, E.P., Karapantsios, T.D., Balouktsis, A.I., Chassapis, D. (2008). Modeling of the optimum tilt of a solar chimney for maximum air flow. *Solar Energy*,

- 82(1): 80-94.
<https://doi.org/10.1016/j.solener.2007.03.001>
- [14] Bassiouny, R., Korah, N.S.A. (2009). Effect of solar chimney inclination angle on space flow pattern and ventilation rate. *Energy and Buildings*, 41(2): 190-196. <https://doi.org/10.1016/j.enbuild.2008.08.009>
- [15] Du, W., Yang, Q.R., Zhang, J.C. (2011). A study of thventilation performance of a series of connected solar chimneys integrated with building. *Renewable Energy*, 36(1): 265-271. <https://doi.org/10.1016/j.renene.2010.06.030>
- [16] Al-Kayiem, H.H., Sreejaya, K.V., Gilani, S.I.U. (2014). Mathematical analysis of the influence of the chimney height and collector area on the performance of a roof top solar chimney. *Energy and Buildings*, 68: 305-311. <https://doi.org/10.1016/j.enbuild.2013.09.021>
- [17] Biwole, P.H., Woloszyn, M., Pompeo, C. (2008). Heat transfers in a double-skin roof ventilated by natural convection in summer time. *Energy and Buildings*, 40(8): 1487-1497. <https://doi.org/10.1016/j.enbuild.2008.02.004>
- [18] Susanti, L., Homma, H., Matsumoto H. (2011). A naturally ventilated cavity roof as potential benefits for improving thermal environment and cooling load of a factory building. *Energy and Buildings*, 43(1): 211-218. <https://doi.org/10.1016/j.enbuild.2010.09.009>
- [19] DeBlois, J., Bilec, M., Schaefer, L. (2013). Simulating home cooling load reductions for a novel opaque roof solar chimney configuration. *Applied Energy*, 112: 142-151. <https://doi.org/10.1016/j.apenergy.2013.05.084>
- [20] Chungloo, S., Limmeechokchai, B. (2007). Application of passive cooling systems in the hot and humid climate: The case study of solar chimney and wetted roof in Thailand. *Building and Environment*, 42(9): 3341-3351. <https://doi.org/10.1016/j.buildenv.2006.08.030>
- [21] Maerefat, M., Haghighi, A.P. (2010). Natural cooling of stand-alone houses using solar chimney and evaporative cooling cavity. *Renewable Energy*, 35(9): 2040-2052. <https://doi.org/10.1016/j.renene.2010.02.005>
- [22] Puangsombut, W., Hirunlabh, J., Khedari, J., Zeghmati, B., Win, M.M. (2007). Enhancement of natural ventilation rate and attic heat gain reduction of roof solar collector using radiant barrier. *Building and Environment*, 42(6): 2218-2226. <https://doi.org/10.1016/j.buildenv.2005.09.028>
- [23] Chang, P.C., Chiang, C.M., Lai, C.M. (2008). Development and preliminary evaluation of double roof prototypes incorporating RBS (radiant barrier system). *Energy and Buildings*, 40(2): 140-147. <https://doi.org/10.1016/j.enbuild.2007.01.021>
- [24] Chungloo, S., Limmeechokchai, B. (2009). Utilization of cool ceiling with roof solar chimney in Thailand: the experimental and numerical analysis. *Renewable Energy*, 34(3): 623-633. <https://doi.org/10.1016/j.renene.2008.05.026>
- [25] Maerefat, M., Haghighi, A.P. (2010). Passive cooling of buildings by using integrated earth to air heat exchanger and solar chimney. *Renewable Energy*, 35(10): 2316-2324. <https://doi.org/10.1016/j.renene.2010.03.003>
- [26] Rabani, R., Faghih, A.K., Rabani, M., Rabani, M. (2014). Numerical simulation of an innovated building cooling system with combination of solar chimney and water spraying system. *Heat and Mass Transfer*, 50(11): 1609-1625. <https://doi.org/10.1007/s00231-014-1366-5>
- [27] Anan-archa, A., Chantawong, P., Khedari, J. (2022). A new configuration of roof skylight combined with solar chimney. *Journal of Engineering Research*. <https://doi.org/10.36909/jer.16259>